Interleukin-6 Enhances Glucose-Stimulated Insulin Secretion From Pancreatic β-Cells

Potential Involvement of the PLC-IP$_3$–Dependent Pathway

Toshinobu Suzuki,[1,2] Junta Imai,[2] Tetsuya Yamada,[1] Yasushi Ishigaki,[2] Keizo Kaneko,[1] Kenji Uno,[2] Yutaka Hasegawa,[2] Hisamitsu Ishihara,[2] Yoshitomo Oka,[2] and Hideki Katagiri[1]

OBJECTIVE—Interleukin-6 (IL-6) has a significant impact on glucose metabolism. However, the effects of IL-6 on insulin secretion from pancreatic β-cells are controversial. Therefore, we analyzed IL-6 effects on pancreatic β-cell functions both in vivo and in vitro.

RESEARCH DESIGN AND METHODS—First, to examine the effects of IL-6 on in vivo insulin secretion, we expressed IL-6 in the livers of mice using the adenoviral gene transfer system. In addition, using both MIN-6 cells, a murine β-cell line, and pancreatic islets isolated from mice, we analyzed the in vitro effects of IL-6 pretreatment on insulin secretion. Furthermore, using pharmacological inhibitors and small interfering RNAs, we studied the intracellular signaling pathway through which IL-6 may affect insulin secretion from MIN-6 cells.

RESULTS—Hepatic IL-6 expression raised circulating IL-6 and improved glucose tolerance due to enhancement of glucose stimulated-insulin secretion (GSIS). In addition, in both isolated pancreatic islets and MIN-6 cells, 24-h pretreatment with IL-6 significantly enhanced GSIS. Furthermore, pretreatment of MIN-6 cells with phospholipase C (PLC) inhibitors with different mechanisms of action, U-73122 and neomycin, and knockdowns of the IL-6 receptor and PLC-β$_1$, but not with a protein kinase A inhibitor, H-89, inhibited IL-6–induced enhancement of GSIS. An inositol triphosphate (IP$_3$) receptor antagonist, Xestospondin C, also abrogated the GSIS enhancement induced by IL-6.

CONCLUSIONS—The results obtained from both in vivo and in vitro experiments strongly suggest that IL-6 acts directly on pancreatic β-cells and enhances GSIS. The PLC-IP$_3$–dependent pathway is likely to be involved in IL-6-mediated enhancements of GSIS. *Diabetes* 60:537–547, 2011

Interleukin-6 (IL-6) is a pleiotropic cytokine produced by several cell types, such as immune cells, adipocytes, myocytes, and endothelial cells. Although IL-6 was initially identified as an immuno-modulatory cytokine secreted from macrophages, several previous studies revealed that IL-6 also has significant impacts on nonimmune events (1), including glucose metabolism.

Obesity is reportedly associated with elevation of circulating IL-6 (2). Functions of IL-6 in insulin-sensitive tissues have been explored by many researchers. There is growing evidence suggesting that IL-6 exacerbates insulin resistance in the liver and adipose tissue, while improving insulin sensitivity in muscle (2). In contrast, the effect of IL-6 on insulin secretion from pancreatic β-cells remains unclear. The IL-6 receptor (IL-6R) was reportedly expressed in murine pancreatic β-cells (3), suggesting a direct impact of IL-6 on pancreatic β-cells. However, a number of controversial in vitro studies demonstrated IL-6 to increase (4,5), decrease (6–8), and have no effect on (9) insulin secretion from isolated pancreatic islets or β-cell lines.

On the other hand, two studies have recently suggested stimulatory effects of IL-6 on insulin secretion in vivo. IL-6 overexpression in muscle, using an electro-transfer method, reduced body fat with liver inflammation and decreased insulin sensitivity in muscle (10). Blood glucose was also shown to be lowered especially in fed states due to enhanced glucose-stimulated insulin secretion (GSIS) in mice, although this study was focused mainly on the liver and muscle (10). In addition, involvement of IL-6 in insulin secretion was recently reported using IL-6-deficient mice (3). High fat (HF)-fed IL-6-knockout (KO) mice displayed no pancreatic α-cell expansion and decreased glucagon levels with impaired GSIS (3). Although the effects of IL-6 on pancreatic α-cell expansion were mainly analyzed, the aforementioned finding prompted us to hypothesize that HF-induced hyperIL-6-emia enhances GSIS. Furthermore, in human subjects as well, association of the plasma IL-6 concentration with first-phase insulin secretion was reported (11). Collectively, chronic elevation of plasma IL-6 concentrations might promote insulin secretion independently of insulin resistance. Therefore, in the current study, to determine the precise role of IL-6 in pancreatic β-cell function, we performed in vivo and in vitro experiments. We first expressed IL-6 in the livers of mice using the adenoviral gene transfer system. Hepatic IL-6 expression raised circulating IL-6 levels accompanied by marked enhancements of GSIS. We also examined the in vitro effects of IL-6 pretreatment on insulin secretion from both pancreatic islets isolated from mice and MIN-6 cells, a murine β-cell line. These experiments showed GSIS enhancement. Finally, we demonstrated that the phospholipase C (PLC)-inositol triphosphate (IP$_3$) dependent pathway is involved in IL-6 enhancement of GSIS in pancreatic β-cells.

RESEARCH DESIGN AND METHODS

Recombinant adenoviruses. Murine IL-6 cDNA was cloned from a liver cDNA library by PCR and ligated into adenovirus vector and then transfected into 293 human embryonic kidney cells. LacZ adenovirus was used as the control (12).

Animals. Animal studies were conducted in accordance with Tohoku University institutional guidelines. We used 8-week-old C57Bl/6N male mice, purchased from Kyudo (Kumamoto, Japan), for in vivo gene transfer study. Mice were housed in an air-conditioned environment, with a 12-h light-dark cycle (light on at 09:00 A.M.), and fed a regular unrestricted diet.

Glucose, insulin, and pyruvate tolerance tests. Glucose tolerance tests (GTT) were performed on fasted (10 h, daytime) mice. Mice were given glucose (2 g/kg of body wt) intraperitoneally, followed by measurement of blood glucose level (13). Insulin tolerance tests (ITT) were performed on ad libitum-fed mice. Mice were intraperitoneally injected with human regular insulin (0.25 units/kg of body wt; Eli Lilly, Kobe, Japan), followed by measurement of blood glucose level (14). Pyruvate tolerance tests were performed on fasted (10 h, daytime) mice. Mice were intraperitoneally injected with sodium pyruvate (2 g/kg of body wt; SIGMA, St. Louis, MO) dissolved in PBS, followed by measurement of blood glucose levels.

Blood analysis. Blood samples were obtained from fasted (10 h, daytime) mice. Blood glucose was assayed with Antsense-III (Horiba Industry, Kyoto, Japan). ELISA kits were used to measure plasma insulin, leptin (Morinaga, Tokyo, Japan), IL-6 (eBioscience, San Diego, CA), adiponectin (Ohtsuka Pharamaceutical, Tokyo, Japan), tumor necrosis factor-α (TNF-α) (R&D Systems, Minneapolis, MN), and glucagon (Wako Pure Chemical, Osaka, Japan) levels. Plasma free fatty acid (FFA) levels were determined with an NEFA C (Wako Pure Chemical, Osaka, Japan) kit. Plasma transaminase levels were determined with a Transaminase C II-test (Wako Pure Chemical, Osaka, Japan) kit.

Immunoblotting. Liver samples obtained from fasted (10 h, daytime) mice were prepared, and tissue protein extracts (250 μg total protein) were boiled in Laemmli buffer containing 10 mmol/L dithiothreitol, subjected to SDS-polyacrylamide gel electrophoresis (15). Antibody to IL-6 (MAB406, R&D Systems) was commercially obtained.

Pancreatic insulin content. Pancreata were suspended in cold acid ethanol (1.5% HCl in 75% ethanol) and minced with scissors, and left at $-20°C$ for 48 h, with sonication every 24 h (16). Insulin contents in the acid ethanol supernatant were determined with an ELISA kit (Morinaga).

Hepatic triglyceride content. Frozen livers were homogenized, and triglycerides were extracted with $CHCl_3:CH_3OH$ (2:1, vol:vol), dried, and resuspended in 2-propanol (14). Triglyceride contents were measured using a Lipidos liquid kit (TOYOBO, Osaka, Japan).

Oxygen consumption. Oxygen consumption was measured with an O_2/CO_2 metabolism measuring system (model MK-5000RQ; Muromachikikai, Tokyo, Japan). Each mouse was kept unrestrained in a sealed chamber with an airflow of 0.5 L/min for 24 h at 25°C. Air was sampled every 3 min, and oxygen consumptions were calculated.

Cell culture. The insulin-secreting β-cell line MIN-6 was maintained in Dulbecco's Modified Eagle Medium containing 25 mM glucose supplemented with 10% fetal calf serum.

Studies with isolated islets and MIN-6 cells. Pancreatic islets were isolated from 8-week-old C57Bl/6N male mice by retrograde injection of collagenase (Sigma) into the pancreatic duct according to the standard procedure as described previously (16). Isolated islets were maintained in RPMI1640 medium containing 11.1 mmol/L glucose. For insulin secretion studies, batches of 10 islets or MIN-6 cells were cultured in the medium under several conditions and then washed with modified Krebs–Ringer bicarbonate buffer (KRBB). After a 30-min preincubation in KRBB containing 1.67 mmol/L glucose, islets or cells were treated for 60 min in KRBB supplemented with either 1.67 or 16.7 mmol/L glucose. Insulin contents of isolated islets or MIN-6 cells were measured after acid ethanol extraction. Recombinant murine IL-6 (PeproTech, London, U.K.), U-73343, U-73122, neomycin (Sigma), Xestospongin C (Biomol, Plymouth Meeting, PA), and H-89 (Millipore, Billerica, MA) were commercially obtained.

Histological analysis. The liver, adipose tissue, and pancreas from LacZ- and IL-6 mice were fixed with 10% formalin, embedded in paraffin, and sectioned. Sections were stained with hematoxylin and eosin. For measurement of β-cell areas, consecutive paraffin sections 500 μm apart spanning the entire pancreas (excised on 14 days after adenoviral treatments) were stained for insulin and with hematoxylin and eosin. After staining, β-cell areas were measured in all sections with Scion Image software (Scion Corporation, Frederick, MD) as described previously (17).

Evaluation of gene expression by RT-PCR. Total RNAs were isolated from 50 mg of hepatic tissue from 10 h-fasted mice on day 5 after adenoviral administration. cDNAs synthesized from 1.0 μg of total RNAs with a First Strand cDNA Synthesis Kit (Roche, Indianapolis, IN) as described previously (18) were evaluated with a real-time PCR quantitative system (Light Cycler Quick System 350S; Roche Diagnostics, Mannheim, Germany), with the oligonucleotides presented in Supplementary Table 1.

The relative amount of mRNA was calculated with β-actin mRNA as the invariant control.

Small interfering RNA transfection. All small interfering RNA (siRNA) oligonucleotides (ON-TARGETplus SMART pool) were purchased from Thermo Fisher Scientific (MA). MIN-6 cells were transfected with siRNAs using DhamaFECT 1 Transfection Reagent (Thermo Fisher Scientific).

Statistical analysis. All data were expressed as means ± SE. For experiments in which data differences needed to be assessed among three or more groups, we used one-way ANOVA followed by Bonferroni's post hoc test. In experiments in which data differences between two groups were assessed, results were analyzed using the unpaired t test.

RESULTS

Adenoviral overexpression of IL-6 elevates plasma IL-6 concentrations and reduces adipose tissue. To explore the role of IL-6 in β-cell function, we prepared recombinant adenovirus containing mouse IL-6 cDNA and injected 3×10^7 PFU IL-6 adenovirus intravenously into C57BL/6N mice (IL-6 mice). Mice administered adenovirus containing the *LacZ* gene were used as controls (LacZ-mice). Immunoblotting of hepatic lysates on day 5 after adenoviral administration confirmed overproduction of IL-6 in the livers of IL-6 mice (Fig. 1A). As reported previously (12,17,19), systemic infusion of recombinant adenovirus resulted in selective transgene expression in the liver with no detectable expression in other tissues (data not shown). Thus hepatic overexpression of IL-6 was achieved and IL-6 produced in the liver was secreted into the systemic circulation, resulting in significant plasma IL-6 elevation, with concentrations peaking at 1,407 ± 368 pg/mL on day 5 after adenoviral administration (Fig. 1B). These plasma IL-6 concentrations in IL-6 mice were within the range of those observed in *ob/ob* and *db/db* mice, murine models of severe obesity (20–22). In contrast, plasma concentrations of TNF-α, another proinflammatory cytokine related to obesity, were similar in these two groups of mice (Fig. 1C). Plasma glucagon concentrations were significantly higher in IL-6 mice (Fig. 1D) than in control mice, which is consistent with the previous report that IL-6 KO mice exhibited low glucagon levels (3). Body weights tended to be reduced in IL-6 mice as compared with those in LacZ-mice and mice without adenoviral administration, although the differences did not reach statistical significance (Fig. 1E). No hepatic architecture changes or cell infiltrations were revealed by histological analyses in IL-6 mice (Fig. 1F). Circulating concentrations of transaminases (Fig. 1G), liver weights (Fig. 1H), and hepatic triglyceride content (Fig. 1I) were similar in IL-6 and LacZ-mice.

Consistent with the findings in mice with IL-6 overexpression in muscle (10), IL-6 mice exhibited reductions in fat masses, i.e., epididymal fat weights (Fig. 2A) and the size of adipocytes, compared with LacZ-mice (Fig. 2B). Daily food intakes of IL-6 mice were decreased (Fig. 2C), and resting oxygen consumptions were significantly increased in IL-6 mice (Fig. 2D). The resultant negative energy balance may explain fat mass reductions. One-shot intracerebroventriclar administration of IL-6 reportedly increased energy expenditure (23) and decreased food intake (24). Because IL-6 reportedly passes across the blood-brain barrier (25), the chronic hyper-IL-6-emia observed in IL-6 mice might affect the central nervous system. Consistent with the fat mass reduction, circulating leptin concentrations were decreased in IL-6 mice (Fig. 2E). However, circulating adiponectin concentrations were decreased in IL-6 mice (Fig. 2F). This result may be explained by the reported finding that IL-6 has an inhibitory effect on adiponectin production by adipocytes (10,26,27).

IL-6 mice exhibit enhancement of GSIS. Next, to explore the impact of circulating IL-6 elevation on glucose metabolism, intraperitoneal GTT were performed on day 5
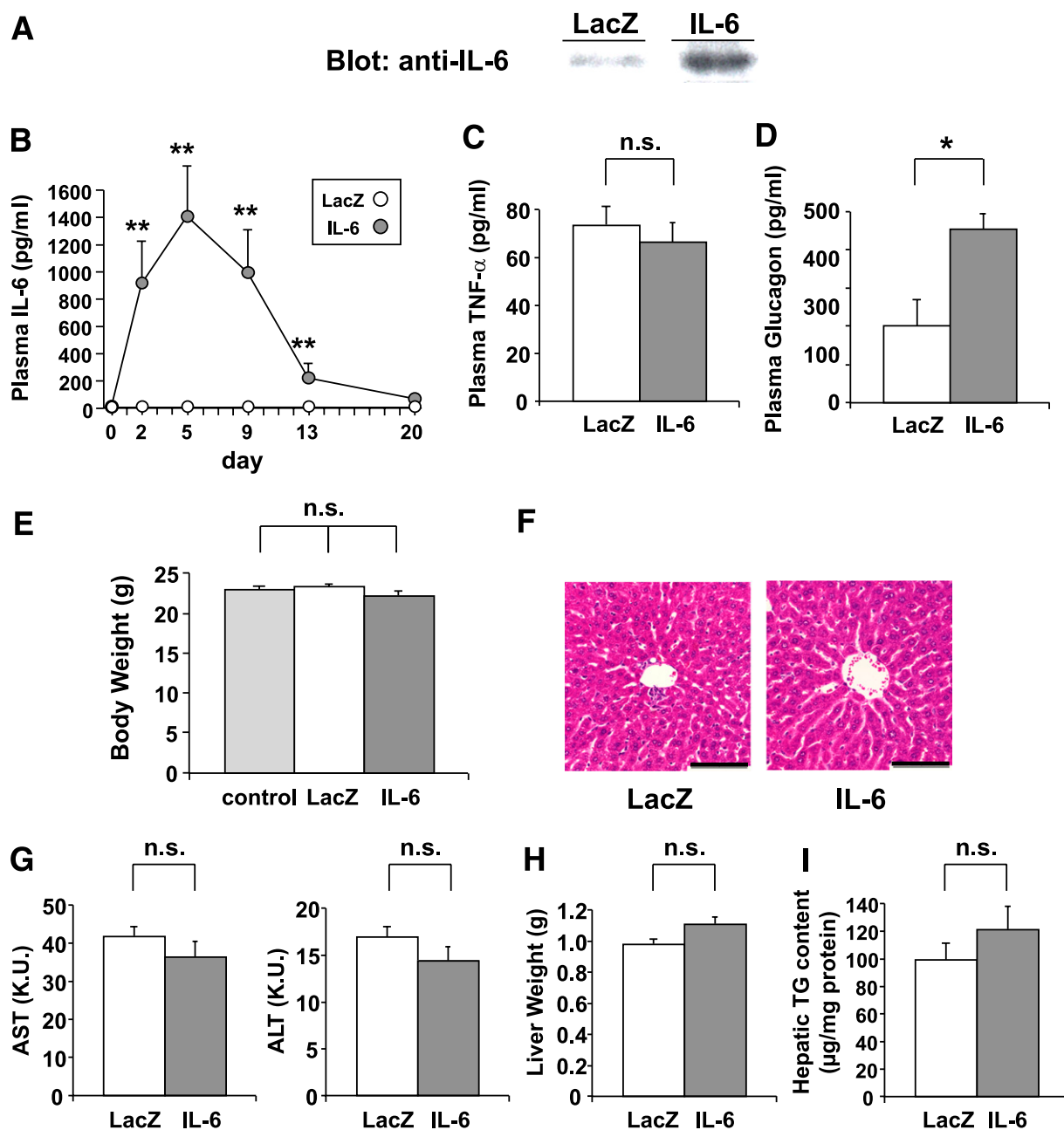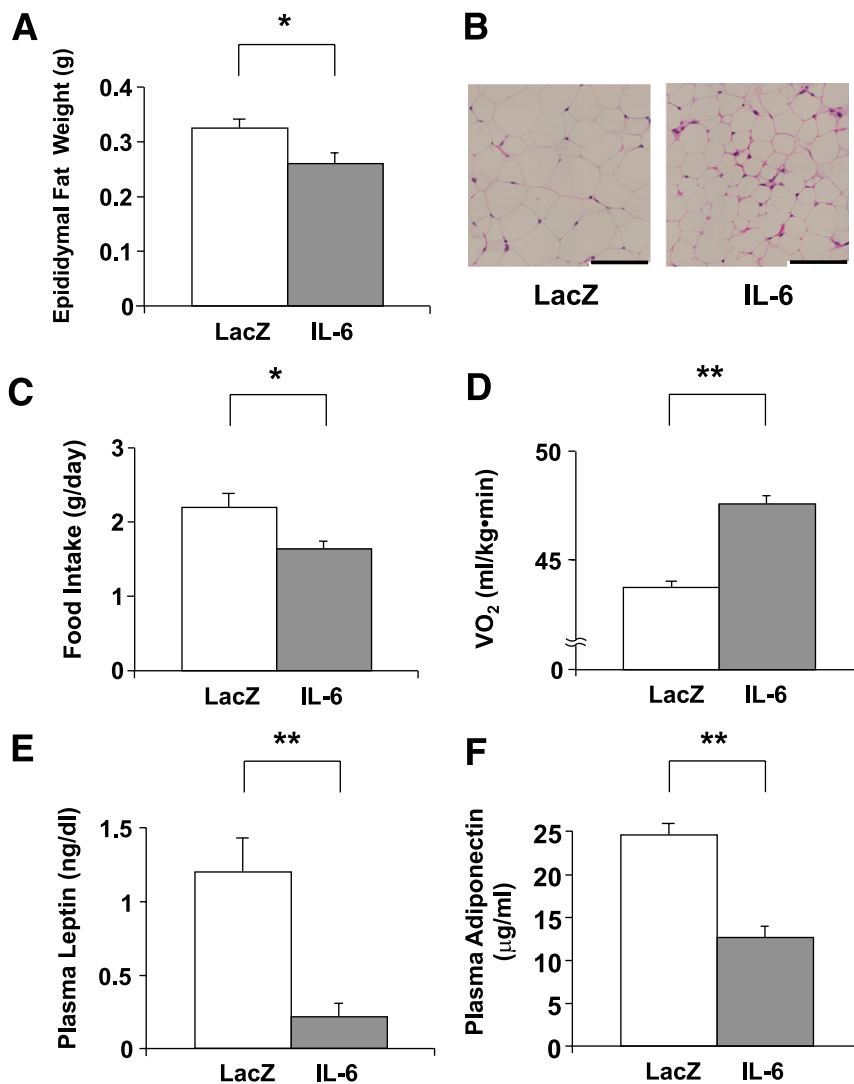
FIG. 1. Adenoviral overexpression of IL-6 raises plasma IL-6 concentrations. Eight-week-old C57Bl/6N male mice were administered adenovirus containing the *LacZ* or the *IL-6* gene. *A*: Immunoblotting of hepatic lysates with anti-IL-6 antibody on day 5 after adenoviral administration. *B*: Plasma IL-6 concentrations were measured in LacZ- (open circles; $n = 5$) and IL-6 (closed circles; $n = 7$) mice through day 20 after adenoviral administration. *C*: Plasma TNF-α concentrations were measured in LacZ- (open bar; $n = 5$) and IL-6 (closed bar; $n = 7$) mice on day 5 after adenoviral administration. *D*: Fasting plasma glucagon levels were measured in LacZ- (open bar; $n = 4$) and IL-6 (closed bar; $n = 4$) mice on day 5 after adenoviral administration. *E*: Body weights of control (not administered adenovirus) (shaded bar; $n = 5$), LacZ- (open bar; $n = 5$), and IL-6 (closed bar; $n = 7$) mice on day 7 after adenoviral administration. *F*: Histological findings of the liver with hematoxylin and eosin staining on day 5 after adenoviral administration. Scale bars indicate 100 μm. *G–I*: Plasma aspartic aminotransferase (AST) and alanine aminotransferase (ALT) levels (*G*), liver weights (*H*), and hepatic triglyceride content (*I*) were measured in LacZ- (open bars; $n = 5$) and IL-6 (closed bars; $n = 7$) mice on day 5 after adenoviral administration. *$P < 0.05$; **$P < 0.01$ vs. LacZ-mice assessed by unpaired t test in *B–D*, *G–I*, and by one-way ANOVA followed by Bonferroni's post hoc test in *E*. Data are presented as means ± SE. (A high-quality digital representation of this figure is available in the online issue.)

after adenoviral administration. IL-6 mice exhibited marked improvement of glucose tolerance compared with LacZ-mice (Fig. 3*A*). Plasma insulin and C-peptide concentrations after glucose loading were remarkably higher in IL-6 mice than in LacZ-mice, whereas fasting insulin and C-peptide levels were similar in these two groups (Fig. 3*B* and *C*). In contrast, ITT revealed no significant difference in insulin sensitivity between these two groups of mice (Fig. 3*D*). These findings indicate that improvement of glucose tolerance, especially after glucose loading, in IL-6 mice is attributable to enhancement of GSIS. On the other hand, pancreatic islet sizes were apparently similar in LacZ- and IL-6 mice (Fig. 3*E*). Quantitatively, β-cell areas (Fig. 3*F*) and pancreatic insulin content (Fig. 3*G*) did not differ between these groups of mice.

Fasting blood glucose levels were also lowered in IL-6 mice, and this effect persisted for 14 days after adenoviral administration (Fig. 3*H*). This result is compatible with the
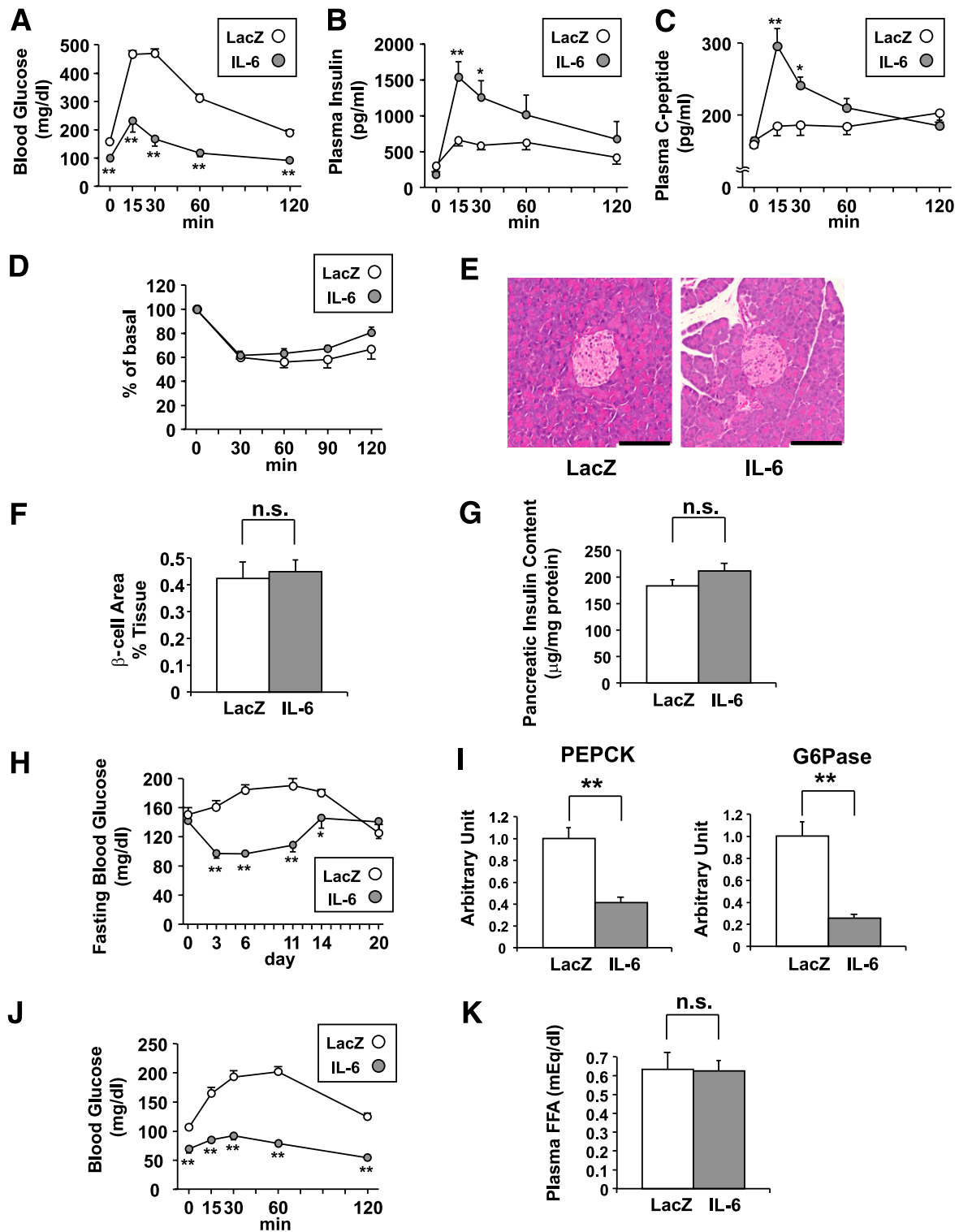
FIG. 2. Adenoviral overexpression of IL-6 reduces adipose tissue. *A*: Epididymal fat weights in LacZ- (open bar; *n* = 5) and IL-6 (closed bar; *n* = 7) mice were measured on day 5 after adenoviral administration. *B*: Histological findings of the epididymal fat tissue with hematoxylin and eosin staining on day 5 after adenoviral administration. Scale bars indicate 100 μm. *C*: Mean daily food intakes for 5 days were calculated in LacZ- (open bar; *n* = 5) and IL-6 (closed bar; *n* = 7) mice. *D–F*: Resting oxygen consumption (*n* = 3 per group) (*D*) and plasma levels of leptin (*E*) and adiponectin (*F*) were measured in LacZ- (open bars; *n* = 5) and IL-6 (closed bars; *n* = 7) mice. *P < 0.05; **P < 0.01 vs. LacZ-mice assessed by unpaired *t* test. Data are presented as means ± SE. (A high-quality digital representation of this figure is available in the online issue.)

exogenous expression period for adenoviral gene transduction (19). IL-6 reportedly activates the signal transducer and activator of transcription-3 (STAT-3) signaling, leading to downregulation of gluconeogenic genes in hepatocytes (28). Consistent with this notion, expressions of gluconeogenic genes, such as phosphoenolpyruvate carboxykinase and glucose-6-phosphatase, were significantly decreased in the livers of IL-6 mice (Fig. 3*I*). In addition, pyruvate tolerance tests revealed that blood glucose levels after pyruvate loading were significantly lower in IL-6 mice than in LacZ-mice (Fig. 3*J*). These findings together indicate that hepatic glucose production was suppressed in IL-6 mice, supporting the previously reported observation that hepatic gluconeogenic gene expressions and fasting blood glucose levels were suppressed in mice with muscle-specific IL-6 overexpression (10).

A lipolytic effect of IL-6 was previously reported (29), and lipolysis raises circulating FFA concentrations. Because FFAs are known to be potent insulinotropic factors (30), we evaluated plasma FFA concentrations. However, plasma FFA concentrations of IL-6 mice on day 5 after adenoviral administration did not differ significantly from those of LacZ-mice (Fig. 3*K*). Thus FFAs are unlikely to be involved in the enhancement of GSIS in IL-6 mice.

IL-6 enhances GSIS from both isolated pancreatic islets and MIN-6 cells. These in vivo findings prompted us to investigate the direct effects of IL-6 on pancreatic β-cells. Therefore, we isolated pancreatic islets from C57BL/6N mice, and the isolated islets were incubated in medium containing 1,200 pg/mL recombinant IL-6 for 48 h, followed by examination of GSIS. Note that the IL-6 concentrations used in these in vitro experiments were similar to the plasma IL-6 concentrations in IL-6 mice on day 5 after adenoviral administration (Fig. 1*B*). At this time point, GSIS enhancements were observed in IL-6 mice (Fig. 3*B*). As shown in Fig. 4*A*, IL-6 pretreatment markedly enhanced insulin secretion in response to 16.7 mmol/L glucose, whereas enhancement of insulin secretion was not statistically significant at 1.67 mmol/L glucose. Pretreatment with IL-6 at a lower concentration, 600 pg/mL,

FIG. 3. Adenoviral overexpression of IL-6 enhances GSIS. *A–C*: Blood glucose (*A*), plasma insulin (*B*), and plasma C-peptide (*C*) levels during glucose tolerance tests performed in LacZ- (open circles; *n* = 5) and IL-6 (closed circles; *n* = 7) mice on day 5 after adenoviral administration. Statistical significance was calculated using the unpaired *t* test. *D*: Blood glucose levels after intraperitoneal insulin injection in LacZ- (open circles; *n* = 5) and IL-6 (closed circles; *n* = 7) mice on day 7 after adenoviral administration. Data are presented as percentages of the blood glucose levels immediately before insulin loading. *E*: Histological findings of the pancreas with hematoxylin and eosin staining on day 5 after adenoviral administration. Scale bars indicate 100 μm. *F*: β-cell areas of LacZ- (open bars; *n* = 5) and IL-6 (closed bars; *n* = 7) mice on day 14 after adenoviral administration. *G*: Pancreatic insulin contents were determined in LacZ- (open bars; *n* = 5) and IL-6 (closed bars; *n* = 7) mice on day 14 after adenoviral administration. *H*: Fasting blood glucose levels were measured in LacZ- (open circles; *n* = 5) and IL-6 (closed circles; *n* = 7) mice through day 20 after adenoviral administration. *I*: Hepatic expressions of PEPCK (*left*) and glucose-6 (*right*) of LacZ- (open bars; *n* = 5) and IL-6 (closed bars; *n* = 7) mice were analyzed by RT-PCR. *J*: Blood glucose levels during pyruvate tolerance tests performed in LacZ- (open circles; *n* = 5) and IL-6 (closed circles; *n* = 7) mice on day 5 after adenoviral administration. *K*: Fasting plasma free fatty acid levels were measured in LacZ- (open bar; *n* = 5) and IL-6 (closed bar; *n* = 7) mice on day 5 after adenoviral administration. *P < 0.05; **P < 0.01 vs. LacZ-mice assessed by unpaired *t* test. Data are presented as means ± SE. (A high-quality digital representation of this figure is available in the online issue.)
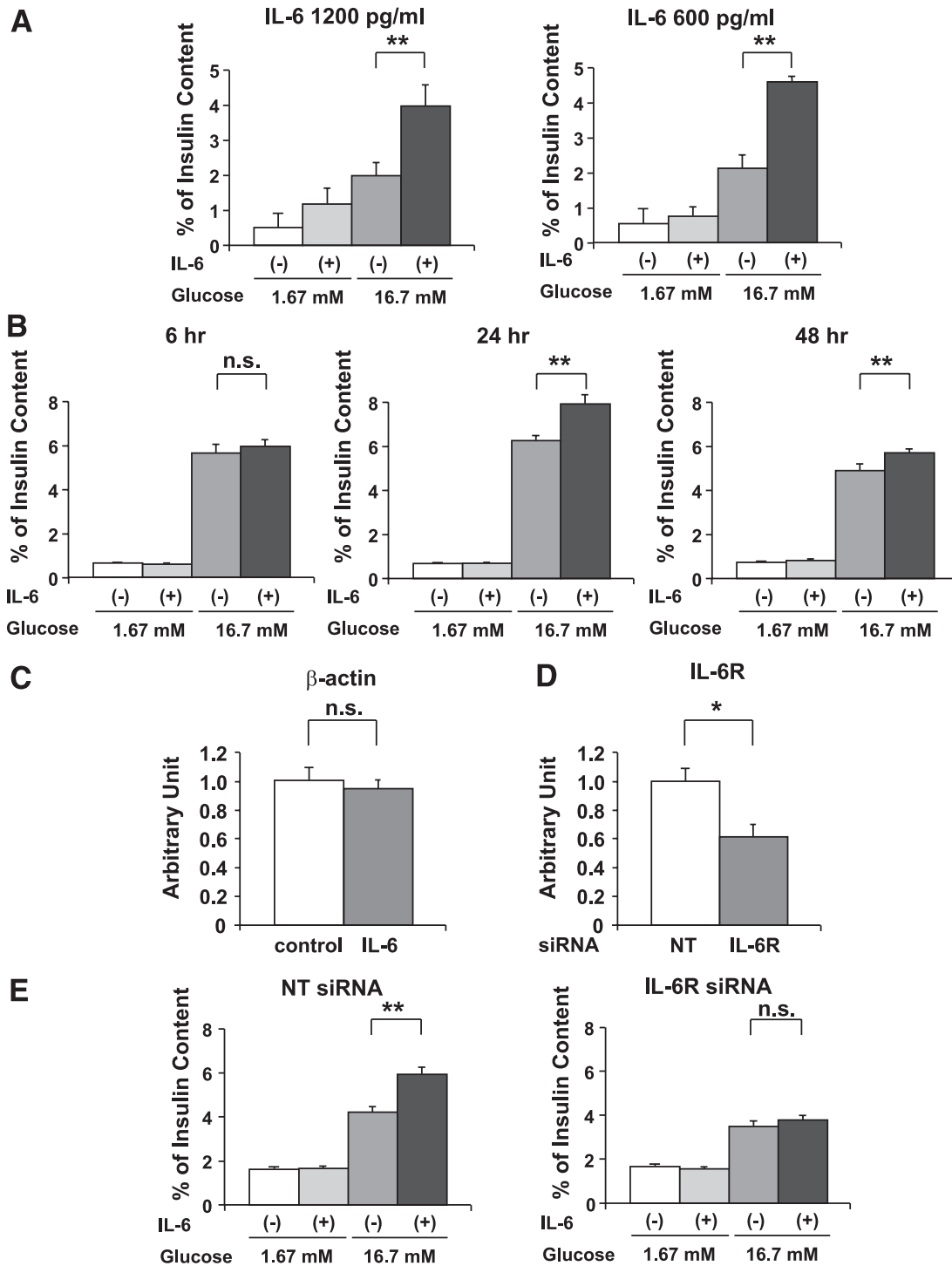
FIG. 4. IL-6 enhances GSIS from both isolated pancreatic islets and MIN-6 cells. *A*: Pancreatic islets were isolated from 8-week-old C57BL/6N mice and then incubated with or without 1,200 or 600 pg/mL recombinant IL-6 for 48 h, followed by examination of insulin secretion for 60 min in KRBB supplemented with either 1.67 or 16.7 mmol/L glucose (*n* = 4 per group). **$P < 0.01$ vs. insulin secretion from islets without IL-6 pretreatment assessed by one-way ANOVA followed by Bonferroni's post hoc test. *B*: MIN-6 cells were incubated with or without 1,200 pg/mL recombinant IL-6 for the indicated periods, followed by measurement of insulin secretion for 60 min in KRBB supplemented with either 1.67 or 16.7 mmol/L glucose (*n* = 6 per group). **$P < 0.01$ vs. insulin secretion from MIN-6 cells without IL-6 pretreatment assessed by one-way ANOVA followed by Bonferroni's post hoc test. *C*: MIN-6 cells were incubated with or without 1,200 pg/mL recombinant IL-6 for 24 h; the cells were used for RT-PCR analysis. β-actin expression levels of MIN-6 cells were quantified and normalized relative to glyceraldehyde-3-phosphate dehydrogenase (GAPDH) mRNA levels. Difference was assessed by unpaired *t* test. *D*: Nontargeting (NT) siRNA (open bars; *n* = 5) or IL-6R siRNA (closed bar; *n* = 5) were applied to the MIN-6 cells. After 48 h incubation, the cells were used for RT-PCR analysis. IL-6R expression levels of MIN-6 cells were quantified and normalized relative to β-actin mRNA levels. *$P < 0.05$ vs. NT siRNA transfected MIN-6 cells assessed by unpaired *t* test. *E*: Knockdown of IL-6R inhibited IL-6-mediated enhancement of GSIS from MIN-6 cells. MIN-6 cells were transfected with NT siRNA or IL-6R siRNA for 24 h and then incubated with or without concomitant 1,200 pg/mL recombinant IL-6 for 24 h, followed by examination of insulin secretion for 60 min in KRBB supplemented with either 1.67 or 16.7 mmol/L glucose (*n* = 5 per group). **$P < 0.01$ vs. insulin secretion from MIN-6 cells without IL-6 pretreatment assessed by one-way ANOVA followed by Bonferroni's post hoc test. Data are presented as means ± SE.

also significantly enhanced GSIS from isolated islets (Fig. 4*A*), although insulin content in isolated islets was not altered by IL-6 pretreatment (Supplementary Table 2). Thus IL-6 directly enhances insulin secretion, particularly in response to a high concentration of glucose.

We further confirmed the direct effect of IL-6 on GSIS using MIN-6 cells, a murine β-cell line that is widely accepted as maintaining glucose responsiveness of insulin secretion in a fashion similar to that in primary pancreatic β-cells (31). MIN-6 cells were incubated in medium containing 1,200 pg/mL recombinant IL-6 for several periods, followed by examinations of GSIS. Although no enhancement of insulin secretion was observed after 6-h incubation with IL-6, significant increments in glucose (16.7 mmol/L)-induced insulin secretion were observed in MIN-6 cells pretreated with IL-6 for more than 24 h, as compared with IL-6-untreated MIN-6 cells. However, no enhancement of insulin secretion was observed at low glucose (1.67 mmol/L) even after 24 h stimulation with IL-6 (Fig. 4*B*). Thus these data clearly showed that IL-6 directly enhances GSIS from pancreatic β-cells. Because a 24-h IL-6-pretreatment period exerted the GSIS-enhancing maximal effect, we performed the following experiments using MIN-6 cells pretreated for 24 h with IL-6 (Fig. 4*B*). Under these conditions, neither insulin content (Supplementary Table 2) nor β-actin expression (Fig. 4*C*) was significantly altered in MIN-6 cells.

Next, to examine whether the effect of IL-6 on enhanced GSIS from MIN-6 cells is actually mediated by the IL-6R, we knocked down IL-6R expression using a specific siRNA. The specific siRNA for the IL-6R significantly reduced expression of IL-6R mRNA in MIN-6 cells (Fig. 4*D*). Suppression of IL-6R expression markedly blunted IL-6-mediated enhancement of GSIS from MIN-6 cells. These findings indicate that the IL-6R is substantially and functionally expressed in MIN-6 cells and that IL-6 exerts its stimulatory effects on GSIS through the IL-6R (Fig. 4*E*).

IL-6–induced enhancement of GSIS is abrogated by PLC pathway inhibitors. Acetylcholine has been shown to enhance GSIS from β-cells, and this GSIS enhancement is mediated, at least partially, by the PLC pathway (32). In addition, IL-6 reportedly activates the PLC pathway in a few other cell types (33,34). Therefore, we next examined involvement of the PLC pathway in IL-6–induced enhancement of GSIS. Isolated pancreatic islets and MIN-6 cells were pretreated with 2 μmol/L U-73122, a PLC inhibitor (35), with or without concomitant 1,200 pg/mL IL-6 for 24 h, followed by measurement of GSIS. As shown in Fig. 5*A* and *B*, IL-6–induced enhancement of GSIS from both isolated pancreatic islets and MIN-6 cells was almost completely abolished with U-73122. We then further confirmed involvement of the PLC pathway in IL-6–induced enhancement of GSIS from MIN-6 cells, using another PLC inhibitor, neomycin. This compound inhibits PLC activity by binding to phosphatidylinositol 4,5-bisphosphatase (PIP_2) (35). Again, pretreatment with 1.5 mmol/L neomycin inhibited IL-6–induced enhancement of GSIS from MIN-6 cells (Fig. 5*C*). Thus two PLC inhibitors, with different mechanisms of action, inhibited IL-6–induced enhancement of GSIS, strongly suggesting that the underlying mechanism is mediated by the PLC pathway.

PLC-β1 is involved in IL-6–induced enhancement of GSIS. To examine which isoform(s) of PLC is involved in IL-6–induced enhancement of GSIS, we knocked down several isoforms of PLC in MIN-6 cells, followed by testing IL-6–induced GSIS. We selected PLC isoforms reportedly expressed in pancreatic islets or a β-cell line (32,36,37) and prepared specific siRNAs for each isoform. Specific siRNAs for PLC-β1, -β2, -β3, -γ1, -γ2, and -δ1 significantly suppressed the expression of each PLC isoform in MIN-6 cells (Supplementary Fig. 1). In addition, knockdown of PLC-$β_1$ and PLC-$γ_1$ was confirmed by immunoblotting (Supplementary Fig. 2). Among them, in PLC-$β_1$-knockdown MIN-6 cells, IL-6 pretreatment did not enhance GSIS (Fig. 5*D*). These results suggest that PLC-$β_1$ is involved in the stimulatory effects of IL-6 on GSIS.

IL-6–induced enhancement of GSIS is not abrogated by a PKA inhibitor. The cyclic AMP (cAMP)-protein kinase A (PKA) pathway, activated by incretins or glucagon, is also well known to enhance GSIS from pancreatic β-cells. Therefore, we next examined the possible involvement of the PKA pathway in IL-6–induced enhancement of GSIS from MIN-6 cells. MIN-6 cells were pretreated with 1 μmol/L H-89, a selective PKA inhibitor (38), with or without concomitant 1,200 pg/mL IL-6 for 24 h, followed by measurement of GSIS. In contrast with the PLC pathway inhibitors, H-89 did not inhibit IL-6–induced enhancement of GSIS from MIN-6 cells (Fig. 6*A*), suggesting a contribution of the cAMP-PKA pathway to IL-6–induced enhancement of GSIS to be unlikely.

IL-6–induced enhancement of GSIS is abrogated by an IP_3 receptor antagonist. The aforementioned results suggest that the PLC pathway is involved in IL-6-mediated enhancement of GSIS. We further examined the downstream pathway from PLC through GSIS enhancement. PLC activation reportedly leads to hydrolysis of PIP_2 into diacylglycerol and IP_3. IP_3 binds to the IP_3 receptor on the endoplasmic reticulum (ER), resulting in the induction of Ca^{2+} release from the ER. This leads to an elevation of the cytoplasmic free Ca^{2+} concentration and subsequently increases insulin secretion (39). To examine whether this mechanism is involved, MIN-6 cells were pretreated with 10 μmol/L Xestospongin C, an IP_3 receptor antagonist (40), with or without concomitant 1,200 pg/mL IL-6 for 24 h, followed by examination of GSIS. Xestospongin C pretreatment decreased insulin content of MIN-6 cells, unlike pretreatments with IL-6, inhibitors, or siRNAs described above (Supplementary Table 2) but did not affect insulin secretion at low (1.67 mM) and high (16.7 mM) concentrations of glucose, when expressed as percentage of insulin content (Fig. 6*B*). In addition, IL-6 pretreatments did not alter insulin content of Xestospongin C-treated MIN-6 cells (Supplementary Table 2). Under these conditions, Xestospongin C inhibited IL-6–induced enhancement of GSIS from MIN-6 cells (Fig. 6*B*). Collectively, these findings indicate that IL-6 directly enhances insulin secretion in response to glucose stimulation through the PLC-IP_3–dependent pathway.

DISCUSSION

IL-6 exerts its effects through binding to a receptor complex consisting of two transmembrane glycoproteins, the specific receptor subunit IL-6R and a 130-kDa signal transducing protein (gp130). Formation of the hexametric IL-6/IL-6R/gp130 complex initiates activation of two major signaling pathways, Janus kinase (JAK)-STAT and the mitogen-activated protein kinase (1). Recently, expressions of both IL-6R and gp130 in murine β-cells were reported, and notably, the expression levels of these molecules were comparable with those in muscle (3), suggesting substantial impacts of IL-6 on pancreatic β-cells. However,
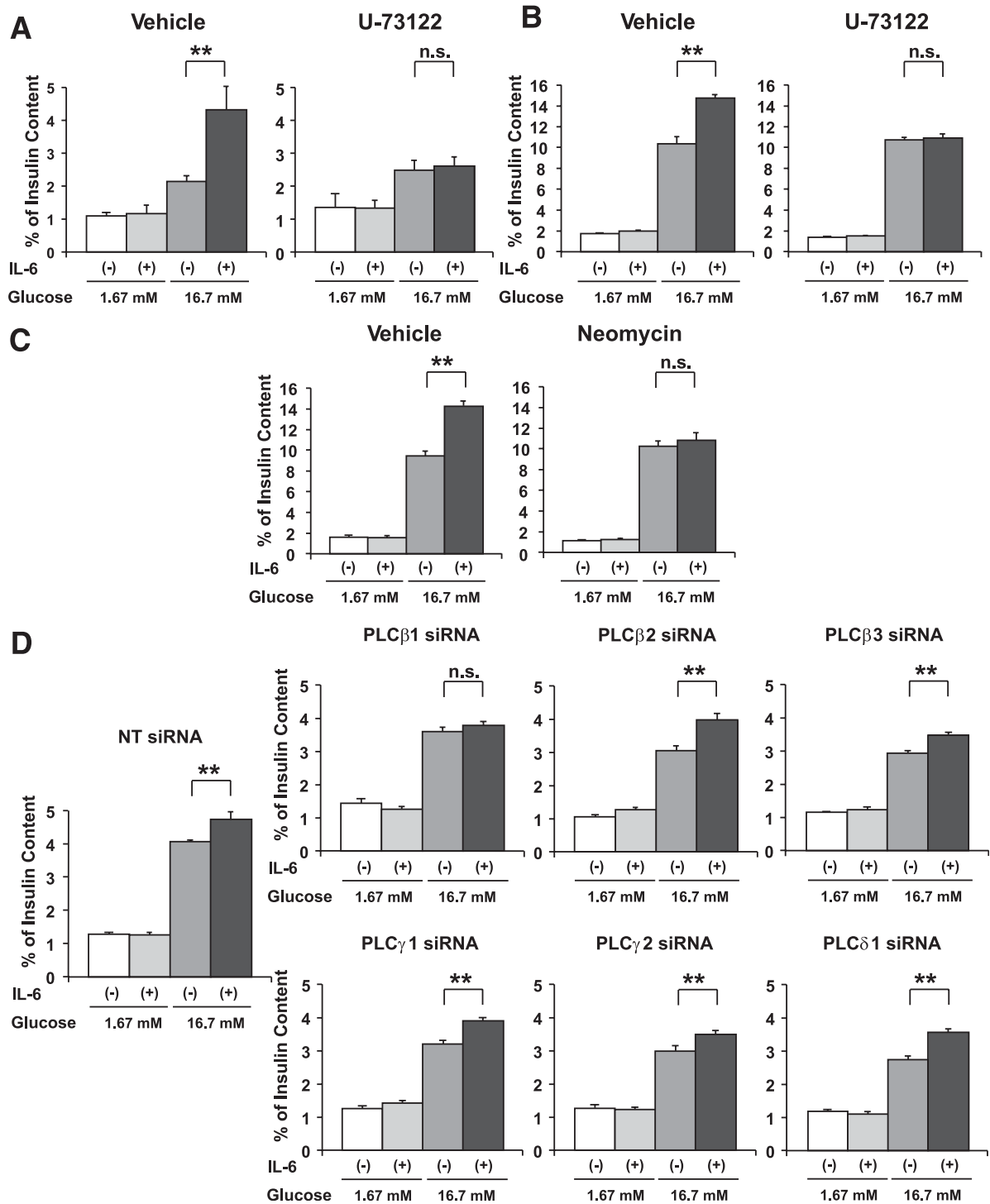
FIG. 5. IL-6 enhances GSIS through the PLC-dependent pathway. *A*: Pancreatic islets isolated from 8-week-old C57BL/6N mice were pretreated with vehicle or 2 μmol/L U-73122 with or without concomitant 1,200 pg/mL IL-6 for 24 h, followed by measurement of insulin secretion for 60 min in KRBB supplemented with either 1.67 or 16.7 mmol/L glucose (n = 5 per group). **P < 0.01 vs. insulin secretion from isolated islets without IL-6 pretreatment assessed by one-way ANOVA followed by Bonferroni's post hoc test. *B* and *C*: MIN-6 cells were pretreated with vehicle or a pharmacological inhibitor (2 μmol/L U-73122 [*B*] 1.5 mmol/L neomycin [*C*]) with or without concomitant 1,200 pg/mL IL-6 for 24 h, followed by measurement of insulin secretion for 60 min in KRBB supplemented with either 1.67 or 16.7 mmol/L glucose (n = 6 per group). **P < 0.01 vs. insulin secretion from MIN-6 cells without IL-6 pretreatment assessed by one-way ANOVA followed by Bonferroni's post hoc test. *D*: MIN-6 cells were transfected with NT siRNA or the specific siRNA for each PLC isoform for 24 h and then incubated with or without concomitant 1,200 pg/mL recombinant IL-6 for 24 h, followed by examination of insulin secretion for 60 min in KRBB supplemented with 16.7 mmol/L glucose (n = 5 per group). **P < 0.01 vs. insulin secretion from MIN-6 cells without IL-6 pretreatment assessed by one-way ANOVA followed by Bonferroni's post hoc test. Data are presented as means ± SE.
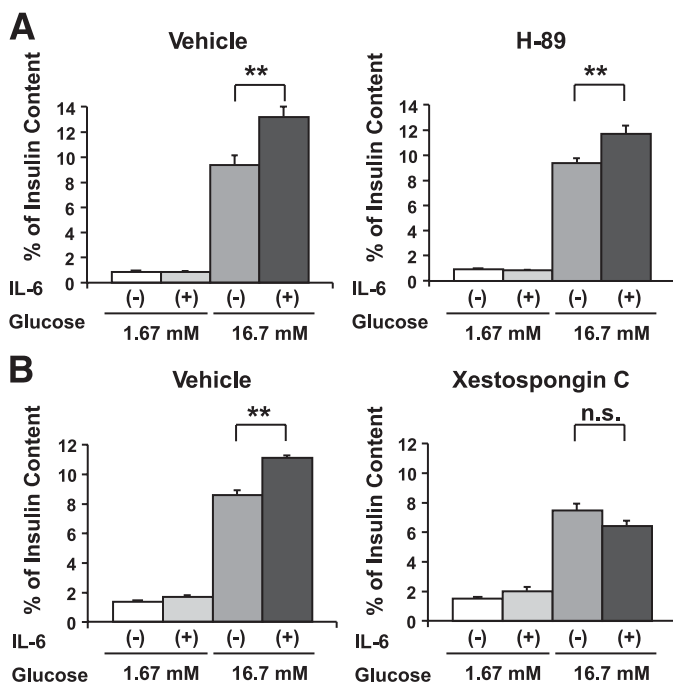
FIG. 6. IL-6–induced enhancement of GSIS is abrogated by an IP_3 receptor antagonist but not by a PKA inhibitor. MIN-6 cells were pretreated with vehicle or a pharmacological inhibitor (1 μmol/L H-89 [A] or 10 μmol/L Xestospongin C [B]) with or without concomitant 1,200 pg/mL IL-6 for 24 h, followed by measurement of insulin secretion for 60 min in KRBB supplemented with either 1.67 or 16.7 mmol/L glucose ($n = 6$ per group). **$P < 0.01$ vs. insulin secretion from MIN-6 cells without IL-6 pretreatment assessed by one-way ANOVA followed by Bonferroni's post hoc test. Data are presented as means ± SE.

consistent effects of IL-6 on insulin secretion have not been reported. At 1,500 pg/mL, IL-6 increased basal insulin secretion from murine isolated islets (4), and at 100 pg/mL, IL-6 increased both basal and glucose-stimulated insulin secretion from HIT-15 cells, a hamster β-cell line (5). On the other hand, 500–2,000 pg/mL (6) or 200–2,000 pg/mL (7) of IL-6 decreased GSIS from rat isolated pancreatic islets and 400 pg/mL IL-6 decreased GSIS from mouse isolated pancreatic islets (8). Furthermore, 400,000 pg/mL IL-6 did not alter insulin secretion from MIN-6 cells (9). Although the reason is unclear, these inconsistencies might be due to the different IL-6 concentrations and preincubation periods as well as sources of pancreatic β-cells used in the experiments. Therefore, in the current study, to elucidate the role of obesity-induced hyper-IL-6-emia in insulin secretion, we focused on IL-6 concentrations within the range of those observed in *ob/ob* and *db/db* mice, 150–7,000 pg/mL (20–22) in both in vivo and in vitro experiments. In addition, a circulating IL-6 level as high as 3,400 pg/mL was reported in obese human subjects (41). In the present in vivo study, plasma IL-6 concentrations were elevated and remained at 900–1,400 pg/mL during first the 10 days after adenoviral IL-6 expression in the liver. We used a similar concentration, 1,200 pg/mL, of IL-6 in our in vitro experiments.

We analyzed IL-6 effects on insulin secretion comparing three different settings of pancreatic β-cells, i.e., murine in vivo, isolated pancreatic islets ex vivo, and a pancreatic β-cell line, MIN-6 cells in vitro. Notably, all experiments showed IL-6–induced enhancement of GSIS, suggesting a direct effect of IL-6 on pancreatic β-cells. In addition, IL-6R knockdown, PLC inhibitors, and an IP_3 receptor

antagonist almost completely inhibited the IL-6–induced enhancement of GSIS. PLC activation reportedly leads to hydrolysis of PIP_2 into diacylglycerol and IP_3. IP_3 binds to the IP_3 receptor on the ER, resulting in the induction of Ca^{2+} release from the ER. This raises the cytoplasmic free Ca^{2+} concentration and subsequently enhances insulin secretion (39). Our findings indicate that activation of the PLC-IP_3–dependent pathway by IL-6 appears to play a major role in GSIS enhancement during hyper-IL-6-emia. Activation of the PLC pathway by IL-6 signaling has been reported in several cell types. For instance, direct association of gp130 and PLC-γ was shown in a Ewing's sarcoma cell line (33). Activation of PLC-γ_1 by IL-6 was also reported in a pheochromocytoma cell line (34). On the other hand, in this study, siRNA experiments revealed knockdown of PLC-β_1, but not other isoforms, significantly to blunt IL-6–induced GSIS. Because the degrees of expression suppression differed among siRNAs specific for each PLC isoform (Supplementary Fig. 1), these results do not exclude the possibility that other PLC isoforms contribute to IL-6-induced GSIS. However, the data strongly suggest involvement of PLC-β_1 itself in the underlying mechanism. PLC-β_1 is reportedly activated by G protein-coupled receptors (42). Taken together with the results that long incubation periods, i.e., 24 h, were required for the stimulatory effects of IL-6 on GSIS, unknown mechanisms involving transcriptional or posttranscriptional alterations in certain molecules might mediate between the IL-6R and G protein-coupled receptor pathways.

Stimulatory effects of IL-6 on GSIS were also suggested in IL-6-KO mice (3). In HF-fed IL-6-KO mice, GSIS was impaired without alterations in pancreatic β-cell mass, resulting in postprandial hyperglycemia. The authors mainly analyzed the effects of IL-6 on pancreatic α-cell expansion, since IL-6-KO mice exhibited low glucagon levels with impaired pancreatic α-cell expansion (3). In the current study, plasma glucagon concentrations were significantly higher in IL-6 mice. In addition, interestingly, IL-6 enhanced GSIS more robustly in vivo and in isolated islets than that in MIN-6 cells (compare Fig. 3B and 4A with 4B). These findings suggest that the effects of IL-6 on glucagon secretion from pancreatic α-cells may have some impact on insulin secretion from β-cells in both in vivo and ex vivo experiments, in addition to the direct effects of IL-6 on β-cells.

Is the observed IL-6–mediated enhancement of GSIS involved in physiological or pathological states? Obesity leads to elevation of circulating IL-6. Circulating IL-6 is reportedly related to fat mass, and this relationship is also observed in mildly obese human subjects (43), suggesting that circulating IL-6 increases in the early phase of obesity. Notably, in human subjects, early in the development of obesity, GSIS is enhanced (44), and insulin hypersecretion occurs before blood glucose elevation (45–47). In mice, IL-6 deficiency reportedly raises postprandial blood glucose levels after HF diet loading (48) mainly due to impaired GSIS (3). In addition, in human subjects, circulating IL-6 concentrations correlate positively with first-phase insulin secretion, and this correlation is independent of insulin resistance (11). Taken together, these observations suggest that the mechanism elucidated in this study might be involved in GSIS enhancement in the early stage of obesity development. We recently identified a neuronal pathway from the liver as being involved in hyperinsulinemia in obese mice (17). In this regard, insulin hypersecretion during obesity development appears to be mediated by both neuronal and humoral signals, which are thought to cooperatively regulate

systemic metabolism (49). These mechanisms likely contribute to maintaining glucose homeostasis during obesity development. Interestingly, during septic shock states, hypoglycemia is commonly observed and this phenomenon is explained by hyperinsulinemia (50,51). It is well-known that IL-6 is markedly elevated during septic shock. Collectively, our findings suggest that hyper-IL-6-emia is involved in the development of hyperinsulinemia in states of both obesity and septic shock.

In conclusion, in vivo, ex vivo, and in vitro experiments consistently demonstrated that IL-6 enhances GSIS from pancreatic β-cells and that this enhancement of GSIS is likely to be mediated by the PLC-IP$_3$–dependent pathway. Modulating the PLC pathway in pancreatic β-cells is a potential therapeutic strategy for achieving efficient postprandial insulin secretion.

ACKNOWLEDGMENTS

REFERENCES

1. Kristiansen OP, Mandrup-Poulsen T. Interleukin-6 and diabetes: the good, the bad, or the indifferent? Diabetes 2005;54(Suppl. 2):S114–S124
2. Hoene M, Weigert C. The role of interleukin-6 in insulin resistance, body fat distribution and energy balance. Obes Rev 2008;9:20–29
3. Ellingsgaard H, Ehses JA, Hammar EB, et al. Interleukin-6 regulates pancreatic alpha-cell mass expansion. Proc Natl Acad Sci USA 2008;105:13163–13168
4. Buschard K, Aaen K, Horn T, Van Damme J, Bendtzen K. Interleukin 6: a functional and structural in vitro modulator of beta-cells from islets of Langerhans. Autoimmunity 1990;5:185–194
5. Shimizu H, Ohtani K, Kato Y, Mori M. Interleukin-6 increases insulin secretion and preproinsulin mRNA expression via Ca²⁺-dependent mechanism. J Endocrinol 2000;166:121–126
6. Sandler S, Bendtzen K, Eizirik DL, Welsh M. Interleukin-6 affects insulin secretion and glucose metabolism of rat pancreatic islets in vitro. Endocrinology 1990;126:1288–1294
7. Southern C, Schulster D, Green IC. Inhibition of insulin secretion from rat islets of Langerhans by interleukin-6. An effect distinct from that of interleukin-1. Biochem J 1990;272:243–245
8. Handschin C, Choi CS, Chin S, et al. Abnormal glucose homeostasis in skeletal muscle-specific PGC-1alpha knockout mice reveals skeletal muscle-pancreatic beta cell crosstalk. J Clin Invest 2007;117:3463–3474
9. Choi SE, Choi KM, Yoon IH, et al. IL-6 protects pancreatic islet beta cells from pro-inflammatory cytokines-induced cell death and functional impairment in vitro and in vivo. Transpl Immunol 2004;13:43–53
10. Franckhauser S, Elias I, Rotter Sopasakis V, et al. Overexpression of Il6 leads to hyperinsulinaemia, liver inflammation and reduced body weight in mice. Diabetologia 2008;51:1306–1316
11. Andreozzi F, Laratta E, Cardellini M, et al. Plasma interleukin-6 levels are independently associated with insulin secretion in a cohort of Italian-Caucasian nondiabetic subjects. Diabetes 2006;55:2021–2024
12. Imai J, Katagiri H, Yamada T, et al. Constitutively active PDX1 induced efficient insulin production in adult murine liver. Biochem Biophys Res Commun 2005;326:402–409
13. Yamada T, Katagiri H, Ishigaki Y, et al. Signals from intra-abdominal fat modulate insulin and leptin sensitivity through different mechanisms: neuronal involvement in food-intake regulation. Cell Metab 2006;3:223–229
14. Uno K, Katagiri H, Yamada T, et al. Neuronal pathway from the liver modulates energy expenditure and systemic insulin sensitivity. Science 2006;312:1656–1659
15. Katagiri H, Asano T, Ishihara H, et al. Overexpression of catalytic subunit p110alpha of phosphatidylinositol 3-kinase increases glucose transport activity with translocation of glucose transporters in 3T3-L1 adipocytes. J Biol Chem 1996;271:16987–16990
16. Ishihara H, Takeda S, Tamura A, et al. Disruption of the WFS1 gene in mice causes progressive beta-cell loss and impaired stimulus-secretion coupling in insulin secretion. Hum Mol Genet 2004;13:1159–1170
17. Imai J, Katagiri H, Yamada T, et al. Regulation of pancreatic beta cell mass by neuronal signals from the liver. Science 2008;322:1250–1254
18. Imai J, Katagiri H, Yamada T, et al. Cold exposure suppresses serum adiponectin levels through sympathetic nerve activation in mice. Obesity (Silver Spring) 2006;14:1132–1141
19. Ishigaki Y, Katagiri H, Yamada T, et al. Dissipating excess energy stored in the liver is a potential treatment strategy for diabetes associated with obesity. Diabetes 2005;54:322–332
20. Harkins JM, Moustaid-Moussa N, Chung YJ, et al. Expression of interleukin-6 is greater in preadipocytes than in adipocytes of 3T3-L1 cells and C57BL/6J and ob/ob mice. J Nutr 2004;134:2673–2677
21. Brun P, Castagliuolo I, Di Leo V, et al. Increased intestinal permeability in obese mice: new evidence in the pathogenesis of nonalcoholic steatohepatitis. Am J Physiol Gastrointest Liver Physiol 2007;292:G518–G525
22. Li M, Kim DH, Tsenovoy PL, et al. Treatment of obese diabetic mice with a heme oxygenase inducer reduces visceral and subcutaneous adiposity, increases adiponectin levels, and improves insulin sensitivity and glucose tolerance. Diabetes 2008;57:1526–1535
23. Wallenius V, Wallenius K, Ahrén B, et al. Interleukin-6-deficient mice develop mature-onset obesity. Nat Med 2002;8:75–79
24. Ropelle ER, Fernandes MF, Flores MB, et al. Central exercise action increases the AMPK and mTOR response to leptin. PLoS ONE 2008;3:e3856
25. Banks WA, Kastin AJ, Broadwell RD. Passage of cytokines across the blood-brain barrier. Neuroimmunomodulation 1995;2:241–248
26. Fasshauer M, Kralisch S, Klier M, et al. Adiponectin gene expression and secretion is inhibited by interleukin-6 in 3T3-L1 adipocytes. Biochem Biophys Res Commun 2003;301:1045–1050
27. Gustafson B, Smith U. Cytokines promote Wnt signaling and inflammation and impair the normal differentiation and lipid accumulation in 3T3-L1 preadipocytes. J Biol Chem 2006;281:9507–9516
28. Inoue H, Ogawa W, Ozaki M, et al. Role of STAT-3 in regulation of hepatic gluconeogenic genes and carbohydrate metabolism in vivo. Nat Med 2004;10:168–174
29. Petersen EW, Carey AL, Sacchetti M, et al. Acute IL-6 treatment increases fatty acid turnover in elderly humans in vivo and in tissue culture in vitro. Am J Physiol Endocrinol Metab 2005;288:E155–E162
30. Itoh Y, Kawamata Y, Harada M, et al. Free fatty acids regulate insulin secretion from pancreatic beta cells through GPR40. Nature 2003;422:173–176
31. Ishihara H, Asano T, Tsukuda K, et al. Pancreatic beta cell line MIN6 exhibits characteristics of glucose metabolism and glucose-stimulated insulin secretion similar to those of normal islets. Diabetologia 1993;36:1139–1145
32. Gilon P, Henquin JC. Mechanisms and physiological significance of the cholinergic control of pancreatic beta-cell function. Endocr Rev 2001;22:565–604
33. Boulton TG, Stahl N, Yancopoulos GD. Ciliary neurotrophic factor/leukemia inhibitory factor/interleukin 6/oncostatin M family of cytokines induces tyrosine phosphorylation of a common set of proteins overlapping those induced by other cytokines and growth factors. J Biol Chem 1994;269:11648–11655
34. Lee YH, Bae SS, Seo JK, Choi I, Ryu SH, Suh PG. Interleukin-6-induced tyrosine phosphorylation of phospholipase C-gamma1 in PC12 cells. Mol Cells 2000;10:469–474
35. Fujiwara K, Maekawa F, Yada T. Oleic acid interacts with GPR40 to induce Ca²⁺ signaling in rat islet beta-cells: mediation by PLC and L-type Ca²⁺ channel and link to insulin release. Am J Physiol Endocrinol Metab 2005;289:E670–E677

36. Kelley GG, Zawalich KC, Zawalich WS. Synergistic interaction of glucose and neurohumoral agonists to stimulate islet phosphoinositide hydrolysis. Am J Physiol 1995;269:E575–E582

37. Gasa R, Trinh KY, Yu K, Wilkie TM, Newgard CB. Overexpression of G11alpha and isoforms of phospholipase C in islet beta-cells reveals a lack of correlation between inositol phosphate accumulation and insulin secretion. Diabetes 1999;48:1035–1044

38. Light PE, Manning Fox JE, Riedel MJ, Wheeler MB. Glucagon-like peptide-1 inhibits pancreatic ATP-sensitive potassium channels via a protein kinase A- and ADP-dependent mechanism. Mol Endocrinol 2002;16:2135–2144

39. Ahrén B. Islet G protein-coupled receptors as potential targets for treatment of type 2 diabetes. Nat Rev Drug Discov 2009;8:369–385

40. Tsuboi T, da Silva Xavier G, Holz GG, Jouaville LS, Thomas AP, Rutter GA. Glucagon-like peptide-1 mobilizes intracellular Ca^{2+} and stimulates mitochondrial ATP synthesis in pancreatic MIN6 beta-cells. Biochem J 2003;369:287–299

41. Teramoto S, Yamamoto H, Ouchi Y. Increased plasma interleukin-6 is associated with the pathogenesis of obstructive sleep apnea syndrome. Chest 2004;125:1964–1965

42. Rebecchi MJ, Pentyala SN. Structure, function, and control of phosphoinositide-specific phospholipase C. Physiol Rev 2000;80:1291–1335

43. Carey AL, Bruce CR, Sacchetti M, et al. Interleukin-6 and tumor necrosis factor-alpha are not increased in patients with type 2 diabetes: evidence that plasma interleukin-6 is related to fat mass and not insulin responsiveness. Diabetologia 2004;47:1029–1037

44. Le Stunff C, Bougnères P. Early changes in postprandial insulin secretion, not in insulin sensitivity, characterize juvenile obesity. Diabetes 1994;43:696–702

45. Dubuc PU. The development of obesity, hyperinsulinemia, and hyperglycemia in ob/ob mice. Metabolism 1976;25:1567–1574

46. Blonz ER, Stern JS, Curry DL. Dynamics of pancreatic insulin release in young Zucker rats: a heterozygote effect. Am J Physiol 1985;248:E188–E193

47. Utzschneider KM, Prigeon RL, Carr DB, et al. Impact of differences in fasting glucose and glucose tolerance on the hyperbolic relationship between insulin sensitivity and insulin responses. Diabetes Care 2006;29:356–362

48. Di Gregorio GB, Hensley L, Lu T, Ranganathan G, Kern PA. Lipid and carbohydrate metabolism in mice with a targeted mutation in the IL-6 gene: absence of development of age-related obesity. Am J Physiol Endocrinol Metab 2004;287:E182–E187

49. Katagiri H, Yamada T, Oka Y. Adiposity and cardiovascular disorders: disturbance of the regulatory system consisting of humoral and neuronal signals. Circ Res 2007;101:27–39

50. Filkins JP. Phases of glucose dyshomeostasis in endotoxicosis. Circ Shock 1978;5:347–355

51. Yelich MR. Effects of naloxone on glucose and insulin regulation during endotoxicosis in fed and fasted rats. Circ Shock 1988;26:273–285